

Electronic Supplementary Information:

Nanoscale transport of energy and mass flux during evaporation of liquid droplets into inert gas: computer simulations and experiments

Robert Hołyst^{*a}, Marek Litniewski^a, Daniel Jakubczyk^b, Marcin Zientara^b, Mariusz Woźniak^b

Parameters used in the simulations

| T_b | $\rho_{liq}(0)$ | $R(0)$ | R_b | R_{el} | $L/2$ | $N/10^6$ | N_1/N_2 |
|-------|-----------------|--------|-------|----------|-------|----------|-----------|
| 0.948 | 0.629 | 26.7 | 150.0 | 125.0 | 167.8 | 2.628 | 0.019 |
| 0.903 | 0.665 | 35.9 | 195.0 | 80.0 | 208.7 | 3.618 | 0.036 |
| 0.851 | 0.704 | 26.8 | 235.0 | 150.0 | 262.7 | 4.775 | 0.012 |
| 0.800 | 0.732 | 26.8 | 260.0 | 150.0 | 285.8 | 4.130 | 0.013 |
| 0.758 | 0.760 | 31.5 | 300.0 | 160.0 | 335.9 | 4.537 | 0.022 |
| 0.713 | 0.783 | 34.0 | 405.0 | 160.0 | 450.8 | 7.082 | 0.018 |

Table 1. The initial equilibrium data of the gas-liquid system for a single component system just before the conversion. At the very beginning of the run ($t=0$) all particles at distance r such that $\rho(r)<0.25$ were converted into the second component particles. The simulation parameters (see also Fig.1): L (size of the simulations box), R_b (radius of a sphere inside the simulation box forming the boundary at which the temperature is set at T_b), R_{el} (is the distance at which particles of the second component are removed from the system). N_1 is the number of particles of the first component which forms a liquid droplet and N_2 is the number of particles of the second component which forms an inert gas. The values of R_{el} applied in simulations were chosen as a compromise between two requirements: the first that R_{el} should be large to keep the non-physical particle far away from the liquid surface in order not to disturb the evaporation process and the second that R_{el} should be as low as possible in order to postpone the moment when the particle disappears (which decreases the influence of the particle erase on the evolution of the whole system). For $T_b = 0.903$ and $\eta = 0.5$ we performed additional simulation run for $R_{el} = 180$. The differences in dR/dt (as in Fig. 5) between the process for $R_{el} = 80$ and $R_{el} = 180$ were well below the level of errors.

The density profiles of the first and second component

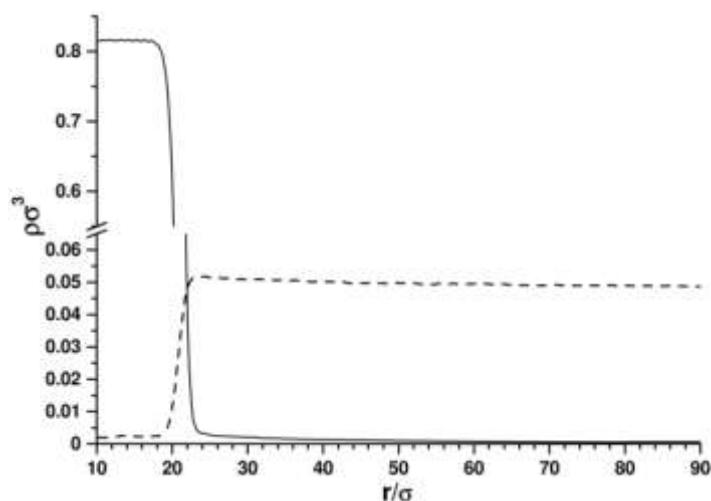


Figure S1. The density profiles during nearly-stationary part of evaporation for $T_b = 0.903$, $\eta = 0.005$. The lines give the densities of the first component (solid) and the second one (dashed). For $r = 80\sigma$ the densities are 0.00055 and 0.0489, respectively.

Temperature and density of the liquid droplet during evaporation

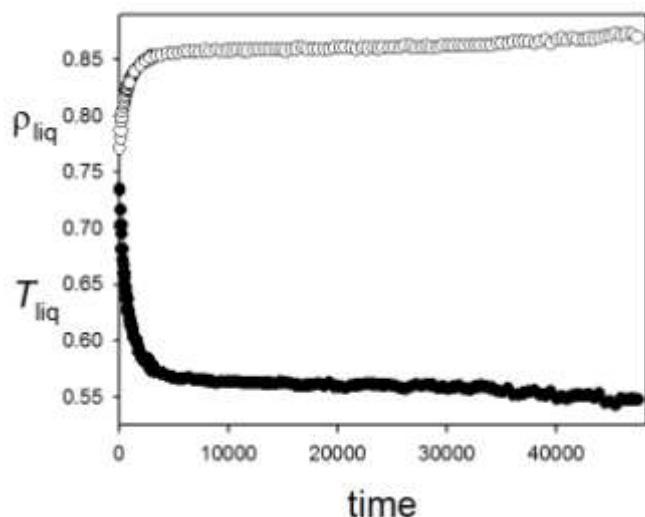


Figure S2. The droplet temperature (filled circles) and the droplet density (empty circles) versus time during the whole evaporation process for $T_b = 0.758$ and $\eta = 0.5$. When a droplet of the same temperature as the temperature of the inert gas is injected into gas it starts to evaporate mostly at the expense of its internal energy. In this way its temperature is reduced from original T_b to T_{liq} . This stage last a short period of time. Later the droplet evaporates at nearly constant temperature. Most of the process of evaporation studied in our paper describes this second quasi-stationary stage of evaporation.

Determination of various parameters (see Eq(11))

| | T_b | η | ρ_b | T_{liq}^R | ρ_{liq}^R | ΔT^{*R} | x_2^R | λ | A |
|---|-------|--------|----------|-------------|----------------|-----------------|---------|-----------|------|
| 1 | 0.948 | 0.5 | 0.0685 | 0.710 | 0.789 | 0.079 | 0.0114 | 2.93 | 0.23 |
| 2 | 0.903 | 0.5 | 0.0484 | 0.668 | 0.808 | 0.181 | 0.0078 | 4.09 | 0.39 |
| 3 | 0.903 | 0.05 | 0.0484 | 0.660 | 0.817 | 0.494 | 0.0003 | 6.69 | 2.16 |
| 4 | 0.903 | 0.005 | 0.0484 | 0.645 | 0.825 | 0.554 | 0.0019 | 9.73 | 2.45 |
| 5 | 0.903 | 0.0005 | 0.0484 | 0.639 | 0.837 | 0.682 | 0.0121 | 14.2 | 2.31 |
| 6 | 0.851 | 0.5 | 0.0327 | 0.627 | 0.831 | 0.335 | 0.0034 | 6.00 | 0.98 |
| 7 | 0.800 | 0.5 | 0.0219 | 0.589 | 0.849 | 0.552 | 0.0025 | 8.78 | 1.87 |
| 8 | 0.758 | 0.5 | 0.0148 | 0.556 | 0.864 | 0.614 | 0.0021 | 12.6 | 1.98 |
| 9 | 0.713 | 0.5 | 0.0096 | 0.524 | 0.879 | 0.725 | 0.0003 | 19.1 | 2.22 |

Table S2. Simulation parameters and results. Index R means the value for $R = 15\sigma$. x_2 is the average number fraction of the first component in the central part of the droplet made of the second component (i.e. $r \leq R - 5\sigma$). Note that because of very low η , the gas for cases n_0 4 and 5 is very close to the perfect gas. Unusual increase in x_2 for n_0 5 is a consequence of very low η , which changes the LJ particles into very small soft spheres. When the mean free path, λ , is small (vapour is dense) A

approaches zero, while for large λ or a vapour forming an ideal gas A approach a constant value 2.2-2.4. In Fig. 4 in the main text we showed cases of vapour being close to the ideal gas.

Determination of the heat conductivity in the vapor

The heat conductivity, κ_v , was measured using a direct method proposed by Muller-Plathe (MP)¹. Differently to original method, in our simulations the amount of kinetic energy, ΔE_k , was transferred (by scaling velocities) between all the particles from the cooling region to the heating one. This enabled us to consider very large systems. The system diameters were many times larger (here, never less than 5) than the mean free path of molecules in the gas. The simulations were performed for total number of particles $N = 256000$ to 384000 . The number increased with decreasing density. The length of the simulation box along the z axis (L_z) was 8.0 – 12.0 times larger than that for x and y (L_x and L_y). The energy transfer was realized for the time interval $\Delta t = 0.8$ or 0.4 . Both the total energy and the momentum of the system were conserved. Mean values of temperature gradient $\partial T/\partial z$ were obtained by fitting the temperature profile $T(z)$ with a straight line (rectangular geometry). For the considered state points any systematic dependence of $\langle \partial T/\partial z \rangle / \Delta E_k$ on ΔE_k was not observed, however the temperature difference between the heating and the cooling region never exceeded $0.2T$. Two independent simulation runs for each state point were performed which enabled us to roughly estimate the error as a difference between the results.

| η | ρ | T | N | L_z/L_x | κ_v |
|--------|--------|-------|--------|-----------|------------|
| 0.5 | 0.0096 | 0.711 | 384000 | 12 | 0.450(6) |
| 0.5 | 0.0149 | 0.756 | 320000 | 10 | 0.473(4) |
| 0.5 | 0.0219 | 0.801 | 256000 | 8 | 0.498(10) |
| 0.5 | 0.0327 | 0.851 | 256000 | 8 | 0.550(8) |
| 0.5 | 0.0685 | 0.948 | 256000 | 8 | 0.655(6) |
| 0.5 | 0.0486 | 0.903 | 256000 | 8 | 0.585(6) |
| 0.05 | 0.0486 | 0.903 | 256000 | 8 | 0.880(9) |
| 0.005 | 0.0486 | 0.903 | 256000 | 8 | 1.19(1) |
| 0.0005 | 0.0486 | 0.903 | 256000 | 8 | 1.74(2) |

Table S3. Thermal conductivity coefficient κ_v for a pure gas at different densities ρ , temperatures T and the values of the energy parameter η . N is the total number of particles used in the simulation. The values in parenthesis give the rough estimation of error in units of the last digit of corresponding value. All expressed in standard L-J units.

The final value of κ_v was evaluated from the formula of MP¹:

$$\kappa_v = \frac{\Delta E_k}{2 \langle \partial T/\partial z \rangle L_x L_y \Delta t} \quad (\text{A1})$$

averaging over all the runs for a given state point. The results are presented in Table S3.

Lewis number and the thermal accommodation coefficient for LJ systems studied.

For different systems we estimated the condensation coefficient (α_C) and the thermal accommodation coefficient α_T together with the Lewis number Le (Table S4 below).

Please note that for the limit of dilute vapor we find $\alpha_C=1$. From the analysis it follows that neither of these quantities can be interpreted in terms of probabilities.

| | T_b | η | T_{liq}^R | ρ_{liq}^R | λ | A | Le | α_T | α_C |
|---|-------|--------|-------------|----------------|-----------|------|------|------------|------------|
| 1 | 0.948 | 0.5 | 0.710 | 0.789 | 2.93 | 0.23 | 1.43 | 14.6 | 10.2 |
| 2 | 0.903 | 0.5 | 0.668 | 0.808 | 4.09 | 0.39 | 1.32 | 8.00 | 6.04 |
| 3 | 0.903 | 0.05 | 0.660 | 0.817 | 6.69 | 2.16 | 1.22 | 1.33 | 1.09 |
| 4 | 0.903 | 0.005 | 0.645 | 0.825 | 9.73 | 2.45 | 1.13 | 1.09 | 0.96 |
| 5 | 0.903 | 0.0005 | 0.639 | 0.837 | 14.2 | 2.31 | 1.13 | 1.16 | 1.02 |
| 6 | 0.851 | 0.5 | 0.627 | 0.831 | 6.00 | 0.98 | 1.29 | 3.11 | 2.40 |
| 7 | 0.800 | 0.5 | 0.589 | 0.849 | 8.78 | 1.87 | 1.23 | 1.55 | 1.26 |
| 8 | 0.758 | 0.5 | 0.556 | 0.864 | 12.6 | 1.98 | 1.24 | 1.48 | 1.19 |
| 9 | 0.713 | 0.5 | 0.524 | 0.879 | 19.1 | 2.22 | 1.24 | 1.31 | 1.06 |

When the vapor becomes dense the A parameter is no longer a constant and starts to depend on thermodynamic state of the system. In fact A should go to 0 for dense vapor but the error in computer simulations is large in this case. Values of α_T and $\alpha_C \sim 1/A$ much larger than 1 are probably due to the fact that the relation between A and the coefficients is no longer correct.

- 1 F. Muller-Plathe, *J. Chem. Phys.* 1997, **106**, 6082.